

## Free convection in a 3D chamber with local cooling and heating

M. Nasiri<sup>a</sup> and B. Ghasemi<sup>a,\*</sup>

<sup>a</sup> Shahrekord University, Department of Mechanical Engineering, Shahrekord, Iran

### Article info:

Received: 07/05/2012  
Accepted: 27/04/2013  
Online: 11/09/2013

### Keywords:

Free convection,  
3D chamber,  
Nusselt number,  
Rayleigh number.

### Abstract

This paper modeled heating air of a room through examining free convection in a 3D chamber. The chamber had cold and hot sources with  $T_c$  and  $T_h$  temperatures, respectively. Its other walls were adiabatic. This study aimed at predicting effect of temperature difference, displacement of hot and cold sources and their aspect ratio on flow field, temperature and heat transfer rate. To conduct the study, mass conservation, momentum and energy equations were applied in laminar and 3D states while assuming fluid constant properties, except density, in the power of buoyancy (Boussinesq approximation). Final difference method (FDM) was used for numerical solution of the governing equations based on the volume control and SIMPLE algorithm. According to the modeling results, the most favorable temperature distribution in the chamber (room) was obtained when the heat source (radiator) was located on the wall under the cold source (window). Reducing the distance between the two sources would result in increasing heat transfer from the heating sources.

### Nomenclature

$A_c$	Cold source area	$T_c$	Cold source temperature
$A_h$	Hot source area	$T_h$	Hot source temperature
$G_r$	Grashof	$T_r$	Base temperature
$g_i$	Acceleration of gravity	$u_c$	Design speed
$g_i$	Cosine of the angle between lines of gravitational field and coordinate axes	$\alpha$	Diffusion coefficient of fluid
$N_u$	Nusselt number	$\beta$	Coefficient of cubical expansion
$n$	Number of knots in the solution mesh	$\zeta$	Compression parameter
$P_r$	Prandtl	$\rho_r$	Density of the fluid at base temperature
$R_a$	Rayleigh number	$v$	Velocity of coefficient of fluid

## 1. Introduction

Buildings are major consumers of energy in the world. Also, heating and cooling equipment and

ventilation systems have a major share in energy consumption of buildings. Prediction of the air flow in buildings and amount of the heat

\*Corresponding author

Email address: ghasemi@eng.sku.ac.ir

and contamination transferred through them can provide very useful information for engineers to optimally design ventilation systems.

Energy consumption in buildings depends on air distribution inside them. As mentioned earlier, choosing a ventilation system capable of consuming the minimum amount of energy which could provide comfort and health for residents is necessary for designing a building. Proper perception of air distribution inside a building (air velocity, temperature distribution, particles distribution) can assist appropriate design of ventilation systems. There are two methods to provide airflow in buildings: experimental method and numerical simulation method.

It is impossible to consider all physical conditions in the numerical simulation; so a series of approximations is needed. Therefore, numerical simulations should be accredited by laboratory results to be used as a standard design. Many numerical and experimental works have been carried out on natural convection flow. Natural convection flow in a chamber was first examined experimentally by Elder [1] and later by Gill and Smide [2]. Water, instead of air, was used in these experiments. Olsen et al. [3] performed an experiment on natural convection flow in an air-containing room using a small model and Rayleigh number of about  $10^{10}$ . Length to height ratio of the room was about 3:1. They showed the measured field flow and temperature within the core and boundary layer. Two side loops were observed in this experiment, which did not exist in the earlier results. This study was one of the few experiments which were carried out in a room with almost real dimensions and conditions.

Among the numerical studies on laminar flow, there is an examination of free convection heat transfer in a tall rectangular chamber with hot surface on the right, cold surface on the left and up and down adiabatic surfaces with Rayleigh numbers of  $10^2$  to  $10^8$  which was done by Yeggmen et al. [4]. Holtzman et al. [5] conducted a similar research in a triangular chamber with hot base and cold adjacent surfaces. Sida and Shohil [6] numerically studied thermal convection of free and laminar

convection in a sloped L-shaped chamber. Using finite difference equations and SIMPLE algorithms, they achieved the average Nusselt number for the variable angles of between zero and 360 degrees, Rayleigh numbers of between 10 and  $10^5$  and length to height ratios of between 1:10 and 1:5. There was also a research by Topo and Zang [7] on temperature and velocity profiles in a laminar and 3D flow inside a cold-surface closed chamber and part of a hot opposite surface with steady heat flux. In this research, a scale was presented to make basic equations of the produced natural flows dimensionless using temperature differences of the opposite surface of the chamber. In another research, Fosegi et al. [8] and Leeputers and Laryant [9] studied heat transfer of free and laminar convection in a cubic chamber. In this chamber, the cold wall, hot wall, boundary conditions and other walls were considered to be on the right, on the left, constant and insulated, respectively. In these studies, they obtained rate of dimensionless heat transfer in the form of average Nusselt number for the Rayleigh numbers of between  $10^3$  and  $10^6$ . Following the above-mentioned works, in the present paper, free convection heat transfer was discussed in a cubic chamber with cold and hot local sources. This study aimed at examining effects of Rayleigh number and dimensions and positions of cold and hot sources on the flow and temperature parameters. This issue, which has been considered less by other researchers, can provide a suitable model for heating a room with windows and radiators.

## 2. Description of the problem

Consider a 3D chamber as shown Fig. 1 in which hot and cold sources are at  $T_h$  and  $T_c$  temperatures, respectively, and other parts are assumed to be insulated.

The heat source can represent a radiator and the cold source a window of the room. The research aimed at studying the effect of temperature difference of the two sources as Rayleigh number, position and dimensional ratio of the heat sources on the basic parameters of temperature and flow. Therefore, in this research, first, the flow field and fluid

temperature of the chamber were obtained using the numerical solution; then, the average Nusselt number, maximum velocity components and average temperature of the chamber were calculated.

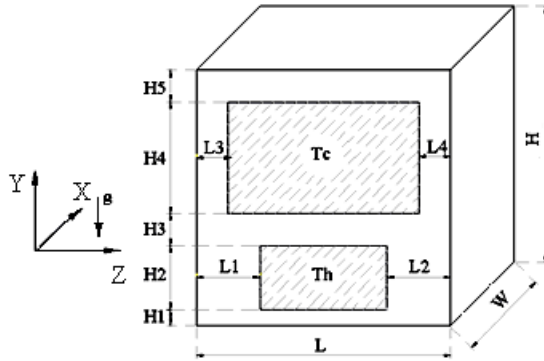


Fig. 1. Geometry of the problem.

### 3. Governing equations

All the basic equations governing the flow of fluid can be categorized into the following groups:

Continuity equation:

$$\frac{\partial(u_j)}{\partial x_j} = 0 \tag{1}$$

Momentum equation:

$$\frac{\partial(u_i u_j)}{\partial x_j} = -\frac{1}{\rho} \frac{\partial p}{\partial x_i} + \frac{\partial}{\partial x_j} \left( \nu \frac{\partial u_i}{\partial x_j} \right) + g_i \tag{2}$$

Energy equation:

$$\frac{\partial(u_j T)}{\partial x_j} = \frac{\partial}{\partial x_i} \left( \alpha \frac{\partial T}{\partial x_j} \right) \tag{3}$$

In the momentum equations,  $g_i$  is acceleration of gravity,  $\nu$  and  $\alpha$  are viscosity and diffusion coefficient of the fluid, respectively. Momentum equations can be expressed more commonly using Boussinesq approximation. Based on this approximation, density of the fluid is constant in all terms, except the buoyancy term. Therefore, pressure can be defined as follows:

$$p' = p + \rho_r g_j x_j \tag{4}$$

where  $\rho_r$  is density of the fluid at the base temperature of  $T_2$ . Knowing thermal coefficient of expansion, buoyancy statement would be as follows:

$$\beta = -\frac{1}{\rho} \left( \frac{\partial \rho}{\partial T} \right)_p = -\frac{1}{\rho} \left( \frac{\rho_r - \rho}{T_r - T} \right) \tag{5}$$

Using Eqs. (4- 5), the following can be given:

$$\frac{\partial p}{\partial x_i} - \rho g_i = -\frac{\partial p'}{\partial x_i} + g_i \rho \beta (T - T_r) \tag{6}$$

In this relation,  $\beta$  is cubical expansion coefficient. In addition, temperature of the cold source ( $T_c$ ) is replaced ( $T_r$ ) as the base temperature. Above relations can be inserted in the momentum equations. Now, to make the equations dimensionless, the following dimensionless numbers could be considered:

$$\begin{aligned} X &= \frac{x}{H} & Y &= \frac{y}{H} & Z &= \frac{z}{H} \\ U &= \frac{u}{u_c} & V &= \frac{v}{u_c} & W &= \frac{w}{u_c} \\ P &= \frac{p}{\rho u_c^2} & \theta &= \frac{T - T_c}{T_h - T_c} \end{aligned}$$

The dimensionless Rayleigh number,  $R_a$ , Prandtl,  $Pr$ , design speed,  $u_c$  and Grashof,  $Gr$  can be expressed as shown below:

$$\begin{aligned} R_a &= Gr_l Pr & u_c &= (g \beta (T_h - T_c) H)^{\frac{1}{2}} \\ Pr &= \frac{\nu}{\alpha} & Gr &= \frac{g \beta (T_h - T_c) H^3}{\nu^2} \end{aligned}$$

Continuity equation:

$$\frac{\partial U_j}{\partial X_j} = 0 \tag{7}$$

Momentum equation:

$$\frac{\partial(U_i U_j)}{\partial X_j} = -\frac{\partial P}{\partial X_i} + \frac{1}{(Gr)^{1/2}} \nabla^2 U_i - \theta g_i^* \tag{8}$$

Energy equation:

$$\frac{\partial(U_j \theta)}{\partial X_j} = \frac{1}{Pr(Gr)^{1/2}} \nabla^2 \theta \tag{9}$$

In these equations,  $g_i^*$  is cosine of the angle between lines of gravitational field and coordinate axes, as follows:

$$g_Z^* = 0, \quad g_X^* = 0, \quad g_Y^* = 1.$$

To examine effect of different parameters on heat transfer rate, local Nusselt number on the thermal sources can be defined using dimensionless numbers:

$$Nu = -\frac{\partial \theta}{\partial X} \tag{10}$$

By integrating the above relations in the hot or cold sources, the average Nusselt number, Num, can be calculated.

$$Nu_{m,c} = \iint_A -\frac{\partial \theta}{\partial X} dA_c \tag{11}$$

$$Nu_{m,h} = \iint_A -\frac{\partial \theta}{\partial X} dA_h \tag{12}$$

where  $A_c$  and  $A_h$  are the cold source area and hot source area, respectively. In addition, average temperature of the chamber can be calculated in each stage as demonstrated by the following equation:

Average temperature:

$$\theta_{maen} = \frac{1}{n} \sum_{i=1}^n \theta_i \tag{13}$$

where  $n$  is number of knots in the solution mesh. The boundary conditions for solving the above equations are as:

On all walls:

$$U_i = 0$$

On hot walls:

$$\theta = 1$$

On cold walls:

$$\theta = 0$$

On adiabatic walls:

$$\frac{\partial \theta}{\partial N} = 0$$

where  $N$  is one of the dimensionless coordination of  $X$ ,  $Y$  and  $Z$ .

#### 4. Solution and control of computer program accuracy

Numerical method of control-volume-based finite difference in an evolving and non-uniform network and SIMPLE algorithm was used to solve Eqs. (7- 9) [10- 11]. A program was provided in Fortran to implement the above algorithm. The equations were solved using line-by-line (LBL) iterative procedure in this program.

Control-volume-based finite difference method was used to convert differential equations into an algebraic form. In this method, the solution field is divided to some control volumes; a control volume encompasses only one knot and the control volumes should not have common volumes. Then, the differential equation is integrated in each of the control volumes. Therefore, the necessary network should be selected in the solution field first. The way of meshing is very effective for the solution method. When an appropriate mesh is not used, it may lead to slow progression and even divergence of the solution. The mesh is compressed near the wall and it is wider at the points located far from it. Different methods are used to make a mesh. In [11], this issue was discussed in detail. In this paper, algebraic method was used to make a mesh. The following relation can be used to make

compression near the wall, e.g.  $Y=0$  and  $Y=H$ :

$$Y = H \frac{(2\alpha + \xi) \left( \frac{\xi + 1}{\xi - 1} \right)^{\frac{\eta - \alpha}{1 - \alpha}} + 2\alpha - \xi}{(2\alpha + 1) \left[ 1 + \left( \frac{\xi + 1}{\xi - 1} \right)^{\frac{\eta - \alpha}{1 - \alpha}} \right]} \quad (14)$$

In this relation,  $\zeta$  is compression parameter. The more  $\zeta$  approaches 1, the more the points would concentrate close to the wall; that is, compression would become more in places close to the wall and it would be less across the mesh and in the middle of the field.  $\eta$  and  $\alpha$  indicate number of divisions and place of compression, respectively. If  $\alpha = 0.5$ , there is uniform compression in  $Y = 0$  and  $Y = H$ .

In order to select an appropriate solution network,  $\xi = 1.01$ , was considered as the optimum amount. Regarding  $\xi = 1.01$  and number of different points in the mesh, the average Nusselt and maximum vertical component of velocity are drawn in Figs. 2-3.

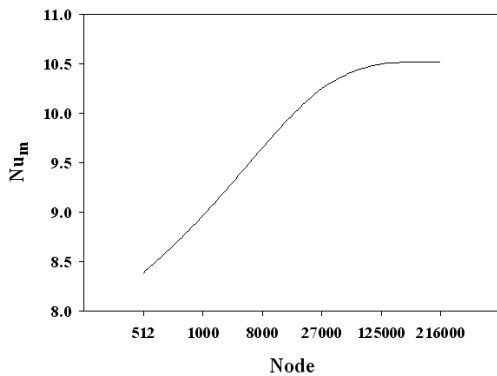


**Fig. 2.** Average Nusselt diagram of hot source in proportion to the number of points of the network ( $Ra=10^5$ ).

Based on the above results and with respect to runtime of the program, the non-uniform  $50 \times 50 \times 50$  mesh was selected for different runtimes of the program.

To examine performance accuracy of the computer code, a comparison was made with activities of previous articles. In these articles, as shown in Fig. 4, a chamber with two vertical opposite walls and two different temperatures was considered. Other walls of the chamber

were insulated.

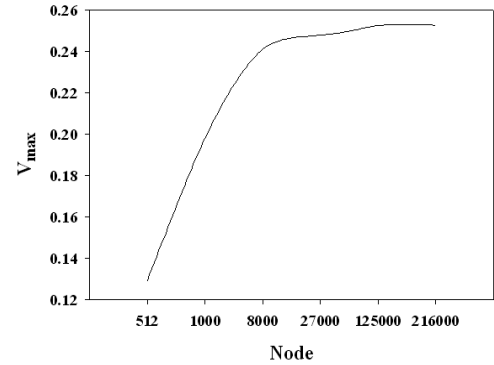


**Fig. 3.** Diagram of maximum vertical component of velocity in proportion to the number of points of the network ( $Ra=10^5$ ).

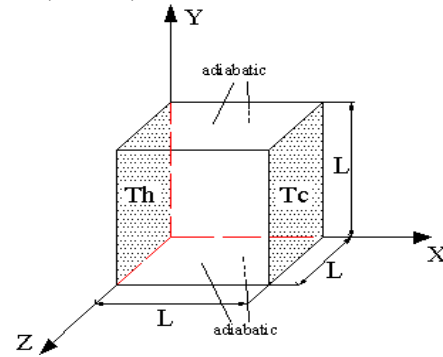


**Fig. 4.** Geometry of the problem to assess authenticity of computer code.

Table 1 shows a sample of comparison, in which the average Nusselt was mentioned in proportion to different Rayleigh numbers. According to this comparison, there is negligible difference between the results.

**Table 1.** Comparing average Nusselt number obtained from the computer program and other works.

Author	$Nu_m$			
	Rayleigh number			
	$10^3$	$10^4$	$10^5$	$10^6$
Present work	1.066	2.039	4.300	8.540
Fusegi et al [8]	1.085	2.001	4.361	8.770
Le putrec and Lauriat[9]	-	-	4.348	8.651
Tou et al. [7]	1.057	2.074	4.367	8.755

**5. Results and discussion**

Different implementations were achieved in different modes after ensuring performance of the computer code and choosing the mesh. Effect of changes of temperature difference related to the sources in the form of the Rayleigh number, displacements and relative size of hot and cold sources on the behavior of fluid was examined in different modes. Constant characteristics of the fluid and chamber dimension  $H=1$ ,  $W=0.875$ ,  $L=1$ ,  $L1=0.3$ ,  $L2=0.3$ ,  $L3=0.2$  and  $L4=0.2$  were considered in all the calculations (Fig. 1).

Examining effect of Rayleigh number;

In this part, only the Rayleigh number was changed. The geometrical parameters including  $H1=0.125$ ,  $H2=0.20$ ,  $H3=0.25$ , and  $H4=0.30$  were supposed to be constant. In this mode, isothermal lines were drawn in Fig. 5 for different Rayleigh numbers in the middle pages,  $Z=0.5$  and  $X=0.4375$ .

As can be observed, for small Rayleigh numbers, the flows caused by the buoyant force were very small and isothermal lines were more regular.

This issue showed that heat transfer in the chamber often occurred in a conductive way. However, with the gradual increase of the Rayleigh number, which happened due to the increased temperature difference, velocity of fluid flow near the thermal surfaces and the curvature of the isothermal lines increased. The velocity of fluid flow near the thermal surfaces led to increase in heat transfer through convection.

The following discussion covers effect of Rayleigh number on heat transfer rate and flow parameters. Figures. 6- 7 show changes of average Nusselt of the heat sources and average temperature in the chamber for changes of Rayleigh number.

As demonstrated in the figures, with the increase of Rayleigh number, the average Nusselt number increased and the average temperature fell in the chamber, which indicated increase of heat transfer rate related to the hot and cold sources.

That would be due to enhancement of the free displacements and consequently increase of velocity components in the chamber. As shown in Table 2, maximum velocity components increased as well, which led to better heat transfer in the chamber.

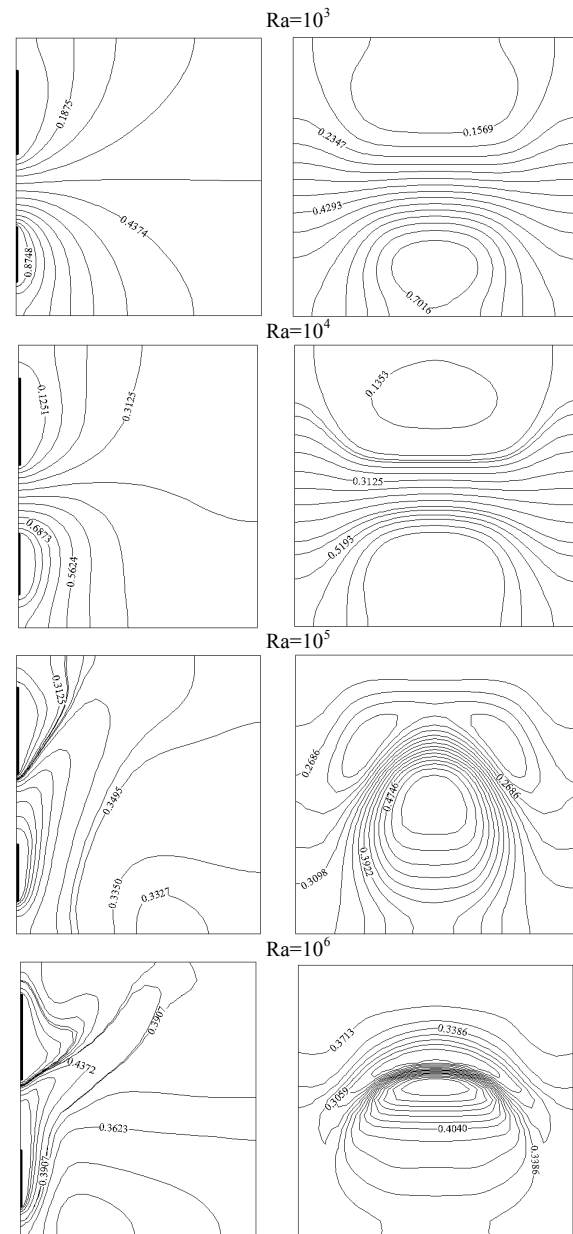


**Fig. 5.** Isothermal lines (right) in part  $X=0.4375$  and isothermal lines (left) in part  $Z=0.5$  for different Rayleigh numbers.

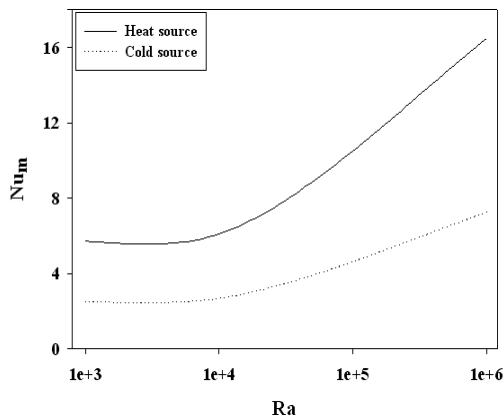


**Fig. 6.** Average Nusselt changes of hot and cold sources in proportion to Rayleigh number changes.

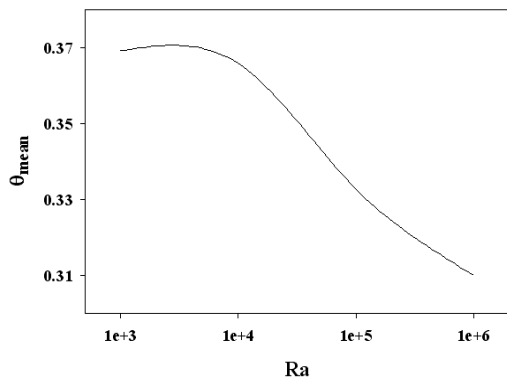


**Fig. 7.** Changes of air average temperature in the chamber in proportion to Rayleigh number changes.

**Table 2.** Comparing maximum velocity components by different Rayleigh numbers.

	Rayleigh number			
	10 <sup>3</sup>	10 <sup>4</sup>	10 <sup>5</sup>	10 <sup>6</sup>
$U_{max}$	0.0217	0.076	0.0824	0.1793
$V_{max}$	0.0269	0.1068	0.2526	0.0735
$W_{max}$	0.0085	0.0577	0.0735	0.1177

Examining position of cold and hot sources; In this part, in addition to changing the distance between the cold and hot sources, H3, here, the sources were placed on the opposite and adjacent walls in two modes. Geometrical parameters of H1=H5, H2=0.20, and H4=0.30 were constant.

Since a laminar flow was assumed in the chamber and according to [3], the Rayleigh

number was considered constant and equal to 10<sup>5</sup> for all these calculations. Fig. 8 shows isothermal lines in this mode in proportion to the displacement of hot and cold sources in the middle plates Y=0.5 and Z=0.5 .

As indicated in diagrams of the figure, when the heat sources were on a wall, reducing the distance between the two sources and their inclination toward center of the plate would lead to increasing compression of the isothermal lines around the heat sources. When the heat sources were placed on the two opposite and adjacent walls, the form of temperature profile would be completely different.

In case the heat sources were placed on the two opposite walls, hot fluid was collected on top of the chamber and cold fluid was collected at its low level.

In case the heat sources were placed on the two adjacent walls, the form of temperature profile would lose its full symmetrical form in proportion to plate Z=0.5.

This discussion is continued by examining effects of displacing heat sources on heat transfer rate and flow parameters.

Figures 9- 11 show heat transfer rate on the hot and cold heat sources in the form of the average Nusselt number, average temperature of the chamber and maximum velocity components in proportion to the distance between the heat sources.

As shown in the diagrams, with the increase of distance between the heat sources, the heat transfer rate considerably decreased in the form of Nusselt number.

As given in Fig. 10, the average temperature of the chamber decreased. If the heat sources were placed far from each other, better displacements would occur because this action would lead in increased maximum velocity components in the chamber (Fig. 11).

Table 3 is provided to study the effect of displacing heat sources on different walls. The table compares heat transfer rate between hot and cold sources and the average air temperature when the distance between them is H3=0.25. The table also shows increase of the average Nusselt when:

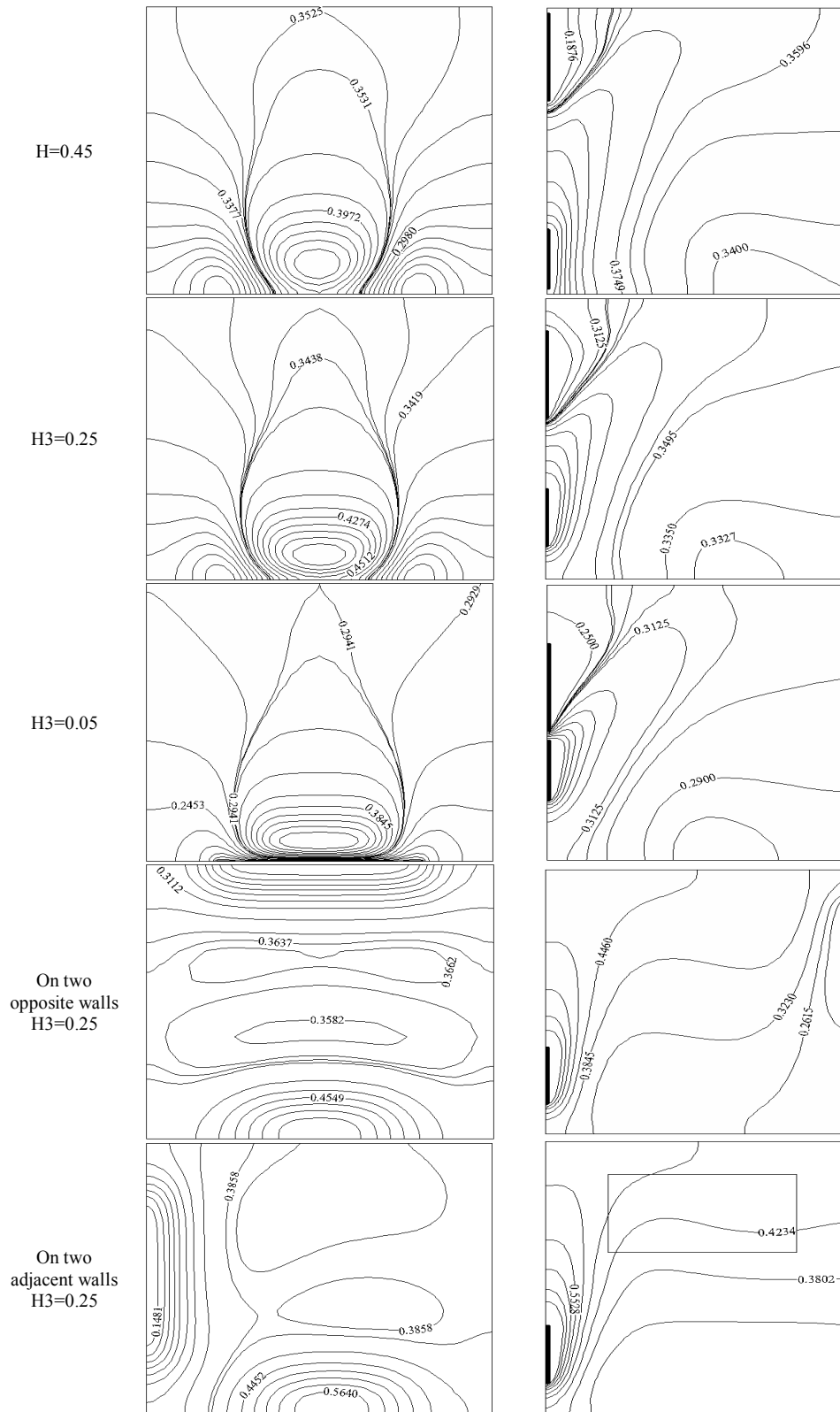


**Fig. 8.** Isothermal lines in part Y=0.5 (right) and isothermal lines in part Z=0.5 (left) in different positions of the sources (Ra=10).

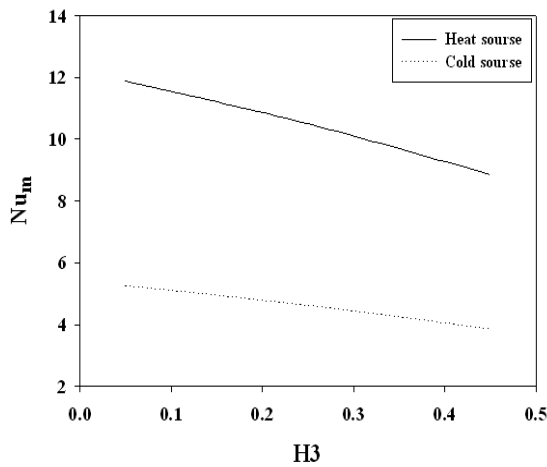


**Fig. 9.** Changes of average Nusselt of hot and cold sources in proportion to changing the distance between heat sources ( $Ra=10^5$ ).

- A) Heat sources were placed on two opposite walls,
- B) Heat sources were placed on the two adjacent walls, and
- C) When they were placed on a wall.

This issue may be attributed to the vortex and regular motion of the fluid, in which the adjacent fluid of the hot source moved up and the adjacent fluid of the cold source moved down the chamber. Here, as the heat sources were placed on the two opposite walls, these two fluids reinforced each other, which led to increase of the average velocity of the heat sources. With the increase of the velocity parameters near the heat sources and due to the fluid displacement, the heat transfer rate increased.

Examining the aspect ratio of hot and cold sources;

The chamber in Fig. 1 was assumed. Maintaining sizes of the hot source, height of the cold source,  $H4$ , was changed. Other geometrical parameters, i.e.  $H1=0.125$ ,  $H2=0.20$  and  $H3=0.25$ , were assumed to be constant. Rayleigh number was be equal to  $10^5$ . Figure 12 shows isothermal lines with respect to the change of height of the cold source in parts  $Z=0.5$  and  $X=0.125$ .

As shown in diagrams of the figure, with the increase of aspect ratio, compression of the isothermal lines gradually increased in regions between the hot sources and the shape of the

temperature profile at the top of the cold source kept a more steady form.

In Fig. 13, the heat transfer rate in the hot and cold sources is shown in the form of the average Nusselt numbers multiplied by the source area.

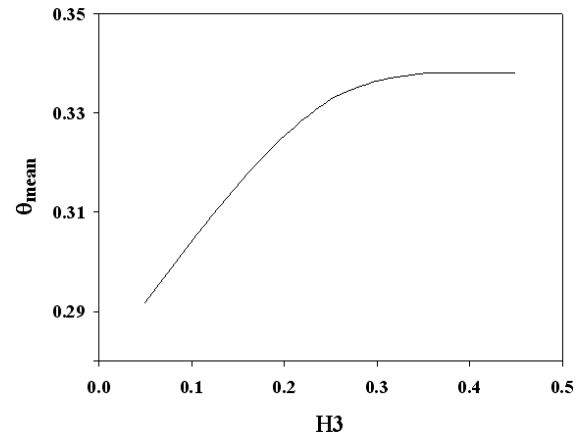


**Fig. 10.** Changes of average temperature in chamber in proportion to changing the distance between heat sources ( $Ra=10^5$ ).

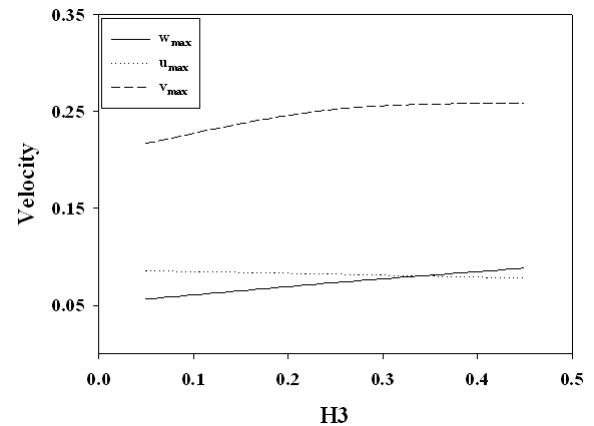


**Fig. 11.** Changes of maximum velocity components in chamber in proportion to changing the distance between heat sources ( $Ra=10^5$ ).

The studies carried out on the changes of aspect ratio of the sources and their effect on the heat transfer rate indicated that, with the increase of the ratio of cold source length to the hot source, according to the related figure, the heat transfer rate was ascended. The reason could be attributed to the increase of maximum velocity components as in Table 4 in directions X, Y and Z.

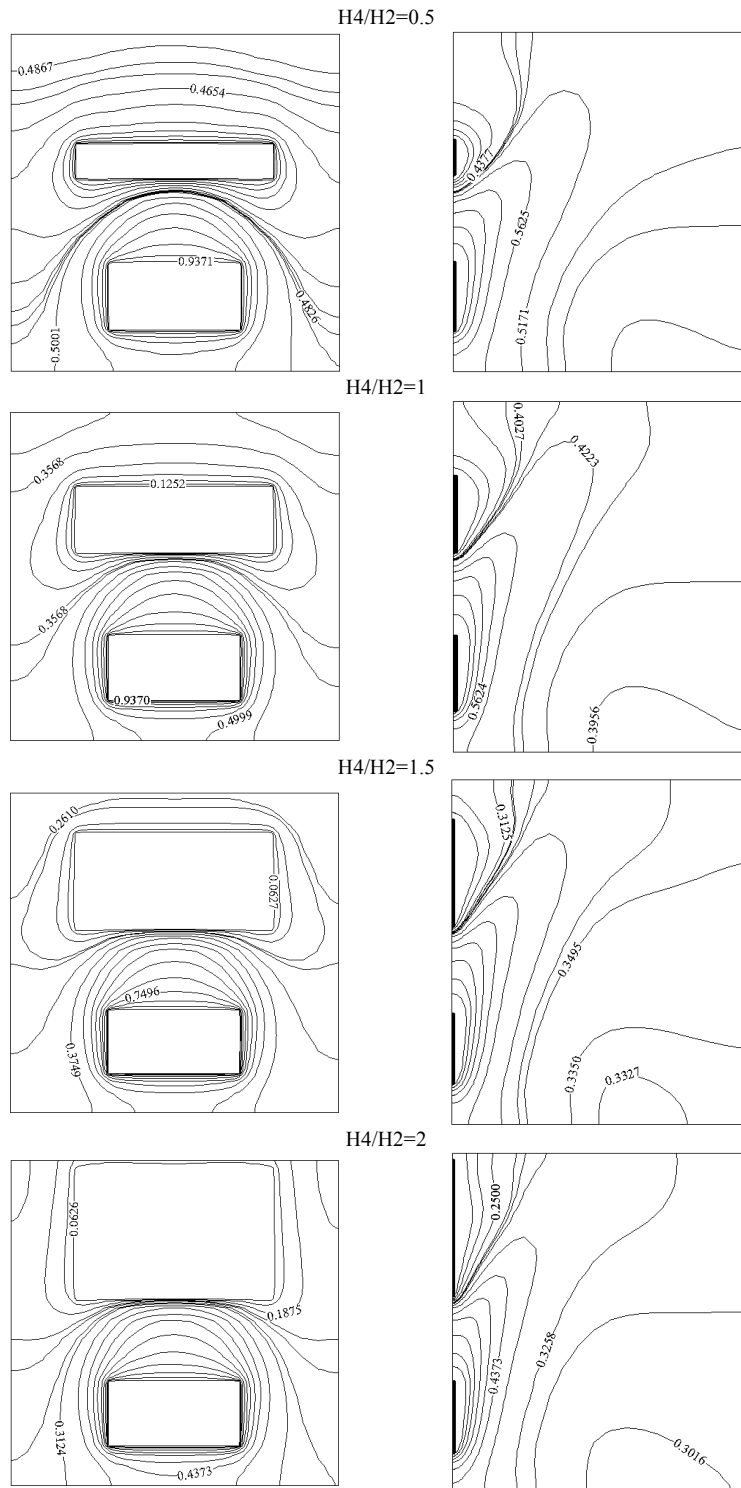


**Fig. 12.** Isothermal lines in part  $X=0.125$  (right) and isothermal lines in part  $Z=0.5$  (left) with different aspect ratios of sources ( $Ra=10^5$ ).

**Table 3.** Heat transfer rate and average temperature of air in different positions of the heat sources.

Heat source displacement	$Nu_{m,h}$	$Nu_{m,h}$	$\theta_{mean}$
On a wall	10.499	-4.620	0.3327
Two opposite walls	11.252	-4.951	0.4516
Two adjacent walls	9.621	-4.622	0.3792

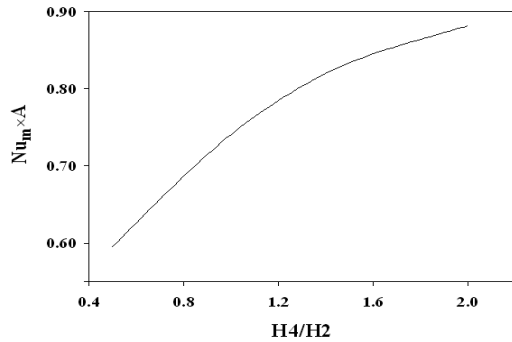


**Fig. 13.** Changes of average Nusselt of hot and cold sources multiplied by source areas in proportion to sources; aspect ratio ( $Ra=10^5$ ).

**Table 4.** Maximum velocity components in different aspect ratios.

	$U_{max}$	$V_{max}$	$W_{max}$
$H4/H2 = 0.5$	0.0620	0.0737	0.2068
$H4/H2 = 1$	0.0675	0.0780	0.2344
$H4/H2 = 1.5$	0.0735	0.0821	0.2526
$H4/H2 = 2$	0.0831	0.0833	0.2622

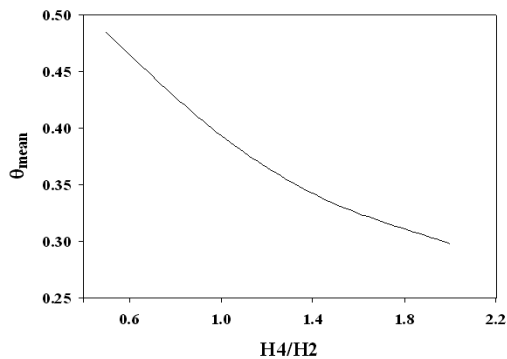


**Fig. 14.** Changes of average temperature of the chamber in proportion to sources' aspect ratio ( $Ra=10^5$ ).

In addition, with the increase of aspect ratio of the cold and hot heat sources, the fall of the average temperature was observed, as given in Fig. 14.

This can be attributed to the increase of the cold source area, which caused fall of temperature in the chamber.

### 6. Conclusions

This paper discussed free convection heat transfer in a 3D chamber with insulated walls and two heat sources placed on the walls. This issue could be a model for heating a room with a window by a heating source, for instance, a radiator. The following results can be presented based on what has been mentioned so far:

If it is assumed that the window and radiator are placed in a fixed position on a wall, with the increase of the Rayleigh number, Nusselt number of the average heat source and maximum velocity components will increase and the average temperature will fall.

Different positions of the window and radiator with fixed dimensions and temperature difference were examined. If the distance between the window and radiator on a wall decreases, the dimensionless heat transfer will increase. In case the window and radiator are placed on the two opposite walls, average Nusselt and average temperature of the chamber will fall.

Different ratios of the window to radiator with temperature difference and fixed distance were also studied. With the increase of the aspect ratio, the dimensionless heat transfer will increase and the average temperature of the chamber will fall.

With respect to the above points, to produce a thermal design, one should pay special attention to choosing window dimensions. Excessive increase in window dimensions causes severe heat loss and fall of room temperature. Besides, position of the heating source of a room, such as a radiator, has a significant effect on optimum heating of the room. Based on the results obtained from this study, it is recommended to place the radiator under a window on a wall while there is short distance between them and consider minimum size for the windows.

**References**

- [1] J. W. Elder, "Turbulence free convection in a vertical slot", *Int. J. Heat Transfer*, Vol. 23, pp. 99-111, (1965).
- [2] P. W. Gie and W. Schmidt, "Experiment study of high Rayleigh number natural convection in an enclosure", *Int. Heat transfer Conf.*, Vol. 4, pp. 1459-1464, (1986).
- [3] D. A. Olsen, L. R. Glicksman and H. M. Ferm, "state natural convection in a empty and partitioned enclosure at high Rayleigh numbers", *Int. J. Heat Transfer, ASME*, Vol. 112, pp. 640-647, (1990).
- [4] J. Xaman, G. Alvavez and C. Estrada, "Numerical study of heat transfer by laminar and turbulent natural convection in tall carities of façade elements", *Energy and Building*, Vol. 37, No. 7, pp. 787-794, (2005).
- [5] G. A. Holtzman, R. W. Hill and K. S. Ball, "Laminar natural convection in isosceles triangular enclosures heated from below and symmetrically cooled from above", *Int. J. Heat Mass Transfer, ASME*, Vol. 122, pp. 477-485, (2000).
- [6] H. T. Syeda and M. Shohel, "Laminar free convection inside an inclined L-shaped enclosure", *Int. J. Heat Mass Transfer*, Vol. 33, No. 8, pp. 936-942, (2006).
- [7] S. K. W Tou and X. F. Zhang, "Three-dimensional numerical simulation of natural convection in an inclined liquid-filled enclosure with an array of discrete heaters", *Int. J. Heat Mass Transfer*, Vol. 46, No. 1, pp. 127-138, (2003).
- [8] T. Fusegi, J. Hyun, M. K. Kuwahara and B. Farouk, "A numerical study of three-dimensional natural convection in a differential heated cubical enclosure", *Int. J. Heat Mass Transfer*, Vol. 34, No. 6, pp. 1543-1557, (1991).
- [9] Y. LePeutrec and G. Lauriat, "Effects of the heat transfer at the side walls on natural convection in cavities", *Journal of Heat Transfer, ASME*, Vol. 112, pp. 370-378, (1990).
- [10] H. K. Versteeg and W. Malalasekera, "An Introduction to Computational Fluid Dynamics", The finite volume method, Henk Kaarle, (1955).
- [11] S. V. Patankar, "Numerical heat transfer and fluid flow", Hemisphere Publication Corporation, Washington, (1980).